

Spontaneous emission in planar semiconductor microcavities displaying vacuum Rabi splitting

I. Abram and J. L. Oudar

*France Telecom/CNET, Centre Paris B, Laboratoire de Bagneux,
196 Avenue Henri Ravera, 92220 Bagneux, France*

(Received 10 June 1994; revised manuscript received 5 December 1994)

We calculate the spontaneous-emission characteristics of a quantum-well exciton embedded in the center of a planar microcavity and compare them with the emission characteristics in a single-mode cavity with lateral confinement of the electromagnetic field. The results indicate that because the modal structure of a planar microcavity consists of a spectrally dense continuum, the exciton decays into the cavity continuum with a time constant close to the free-space spontaneous-emission lifetime, even under conditions in which its spectrum displays the vacuum Rabi splitting. This behavior contrasts with the case of cavities with lateral in-plane confinement of the field, in which the vacuum Rabi splitting is the signature of a dramatic modification of the spontaneous-emission lifetime. The technological implications of this difference are discussed.

PACS number(s): 42.50.-p, 71.35.+z, 73.20.Dx, 78.45.+h

I. INTRODUCTION

The spontaneous-emission characteristics of rare-earth ions or semiconductors in planar microcavities have been a very active field of investigation over the past few years [1–8]. Recently, a splitting has been observed in the absorption and the reflection spectra of quantum-well excitons placed in the center of a resonant epitaxially grown planar microcavity and has been interpreted as representing the vacuum Rabi splitting of the exciton resonance [9,10]. By analogy to what is observed in cavity quantum electrodynamics (CQED) experiments involving a single atom (or a few atoms) in a single-mode cavity [11], this splitting should attest to the strong (polaritonlike) coupling between the main optical mode of the cavity and the excitons in the semiconductor, thus opening the way to the exploitation of CQED effects in technologically important situations, such as the possibility of fabricating thresholdless quantum-well vertical-cavity surface-emitting microlasers or single-mode highly efficient light-emitting diodes.

One way of visualizing why the “strong-coupling” situation can improve the efficiency of semiconductor light emitters is outlined in Fig. 1. Consider two subsystems (the exciton and the cavity) each coupled to a different decay channel. The exciton decays at a rate γ through quasiomnidirectional spontaneous emission, while the field in the cavity gives rise to a light beam directed along the cavity axis with a decay constant of κ for the energy flow. If the exciton is strongly coupled to the cavity (i.e., the Rabi splitting g satisfies $g \gg \kappa, \gamma$), the energy oscillates between the two subsystems at the Rabi angular frequency g , so that in effect it spends half its time in each of the two subsystems. If the cavity lifetime is much shorter than the exciton spontaneous-emission time ($\kappa \gg \gamma$), then practically all the energy stored in the excitons will be channeled to the directional beam emerging from the cavity. For this reason, the strong optical coupling between a semiconductor and a cavity has been thought to

provide an attractive alternative to the recent proposals for controlling spontaneous emission that require difficult fabrication techniques, such as the photonic band-gap structures [12].

There is an important difference, however, between the spherical mirror cavities used in atomic CQED experiments and the planar Fabry-Pérot semiconductor microcavities that can be readily fabricated by standard semiconductor-growth techniques: The former are essentially single-mode cavities, even when they involve imperfect mirrors and transverse (lateral) leakage channels, while the latter are intrinsically multimode with a spectrally dense continuum of modes, even when their mirrors are perfect and lossless. Because of this fundamental difference, the simple intuitive images that have been developed through the physical understanding of CQED phenomena cannot be applied in a straightforward way to

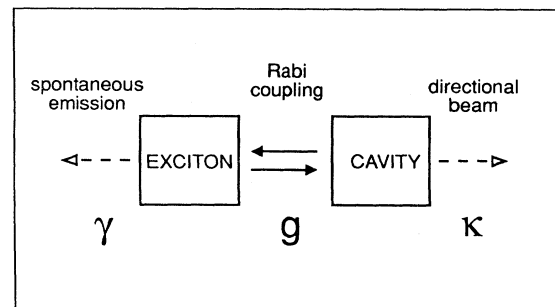


FIG. 1. Schematic representation of the flow of energy in the presence of strong Rabi coupling between an exciton and a single-mode cavity: The exciton decays through spontaneous emission at a rate γ , while the cavity field decays at a rate κ by producing a directive beam. When the Rabi oscillation of the energy between the two subsystems is faster than the two decays ($g \gg \gamma, \kappa$) the combined system will decay at a rate $(\gamma + \kappa)/2$ through the faster of the two decay channels.

the planar microcavity situation; they must be modified by taking explicitly into consideration the continuum of modes of the planar cavity, thus giving sometimes qualitatively different results.

In this paper, we examine an important consequence of the different modal structures of the two types of cavities in relation to the modification of the spontaneous-emission radiation pattern and lifetime, a phenomena that is important for the initiation of laser action in microcavities. We show that although excitons in both types of cavities may present similar splittings in their absorption or reflection spectra, their spontaneous-emission properties are quite different. In particular, single-mode microcavities may induce a dramatic modification of the spontaneous-emission dynamics and thus permit a preferential channeling of spontaneous emission into a directional beam, as discussed above, while, by contrast, planar microcavities cannot increase significantly the fraction of the light intensity emitted spontaneously into the main cavity mode through the sole action of a Rabi coupling mechanism. In pursuing this demonstration, we first review the theory describing the splitting in the reflection or the absorption spectrum of an exciton system placed inside an optical cavity and then examine the expressions for the exciton lifetime both in a single-mode and in a planar microcavity. The characteristics of the spontaneous emission of the excitons are examined by calculating the radiation reaction at the site of the emitting dipole.

A few comments are in order at this point regarding the radiation reaction viewpoint for the treatment of spontaneous emission. Most calculations on spontaneous emission adopt the "vacuum fluctuations" viewpoint whereby the emission rate is evaluated by calculating the coupling of the emitting dipole to the vacuum field of all the radiation modes of the cavity. As a first step, this calculation requires a complete modal analysis of the structure, a procedure that may prove to be a formidable task for any realistic geometry (for example, in the presence of Bragg mirrors). From the radiation reaction viewpoint, on the other hand, the spontaneous-emission characteristics of an emitting dipole are obtained by calculating its radiation pattern under the boundary conditions of the cavity [6,11,13]. From this viewpoint, the spontaneous-emission rate is determined by the value of the electric field produced by the emitter at its own site, that is, by the "radiation reaction." The results obtained in the radiation reaction viewpoint and their range of validity are precisely the same as those obtained in the vacuum fluctuations viewpoint [14,15]. The main advantage of the radiation reaction viewpoint for the calculation of spontaneous emission in cavities with complicated modal structures is essentially computational: since all calculations are performed in direct space, they are well suited to treating the emission of point dipoles and correspond to dealing with all the modes of the field simultaneously. In addition, the calculation of the radiation pattern of the emitting dipole can rely on the vast arsenal of methods that have been developed in classical antenna theory.

The paper is organized as follows. In Sec. II we give a brief review of the theory that describes the vacuum Rabi

splitting in terms of the linear dispersion characteristics of the material system included in the cavity. In Sec. III we develop the theory of the vacuum Rabi splitting of an exciton placed in a single-mode cavity through the dynamical equations for the dipolar emission of the exciton. In Sec. IV we examine the spontaneous emission of an exciton in a planar microcavity whose characteristics are similar to those used in recent experiments for the observation of the exciton splitting. Finally, in Sec. V we summarize our results and review our conclusions.

II. VACUUM RABI SPLITTING AS A FEATURE OF LINEAR-DISPERSION THEORY

The transmission and the reflection spectra of an optical cavity containing a medium that displays a sharp excitonic (or atomic) resonance at $\Omega = 2\pi c/\lambda_0$ have been derived quite simply by invoking the classical theory of linear dispersion [16]. In this section we give a short review of the linear dispersion theory of the Rabi splitting in which we neglect, for simplicity, the cavity decay or, equivalently, its spectral linewidth.

The resonance condition for an electromagnetic wave of wavelength $\lambda = 2\pi c/\omega$ propagating along the axis of a (confocal or planar) cavity is that the cavity length L should be equal to a half-integral number of wavelengths

$$L = \frac{m}{2} \frac{\lambda}{n}, \quad (1)$$

where $m = 1, 2, 3, \dots$ while n is the refractive index of the material in the cavity. In our case, n is given by

$$n = n_0 \left\{ 1 - \frac{\alpha_0 c}{\Omega} \frac{(\omega - \Omega)\gamma/2}{(\omega - \Omega)^2 + (\gamma/2)^2} \right\}, \quad (2)$$

where n_0 is the "background" dielectric constant of the medium (i.e., in the absence of the exciton resonance), while α_0 is the absorption coefficient at the peak of the exciton resonance that corresponds to a Lorentzian line of width γ .

If the cavity length is adjusted to

$$L = \frac{m}{2} \frac{\lambda_0}{n_0} \quad (3)$$

so that the transmission peak of the "cold" cavity is at the same wavelength as the exciton absorption, the resonance condition (1) in the vicinity of the exciton transition ($\omega \approx \Omega$) can be rewritten as

$$\omega - \Omega = \alpha_0 c \frac{(\omega - \Omega)\gamma/2}{(\omega - \Omega)^2 + (\gamma/2)^2}, \quad (4)$$

giving the familiar double-peaked spectrum with maxima at

$$\omega = \Omega \pm \sqrt{\alpha_0 c \gamma/2 - (\gamma/2)^2}. \quad (5)$$

This simple theory for the absorption and reflection spectra of atoms (or excitons) in resonant cavities is valid for both single-mode and planar cavities. It has been successfully applied to account for the spectral doublet observed both in atomic CQED experiments [16] and, more

recently, in the absorption and reflection spectra of quantum-well excitons in planar microcavities [9,10].

III. SPONTANEOUS EMISSION IN SINGLE-MODE MICROCAVITIES

We consider a harmonic oscillator placed at the origin of a Cartesian coordinate system and interacting with the electromagnetic field through a dipolar transition. The transition dipole μ can be taken to lie along the \hat{x} axis, while the confinement of the field in the cavity occurs mainly along the \hat{z} axis (see Fig. 2). The harmonic oscillator may represent a collection of two-level atoms (in the limit of very weak excitations) or a system of excitons in a semiconductor. As the aim of this paper is to discuss the properties of semiconductor microcavities, we shall refer to the harmonic oscillator as an "exciton." Within the radiation reaction viewpoint, the spontaneous-emission rate is determined by the electric field that the emitter produces at its own site. Although a rigorous quantum-mechanical formulation of this viewpoint is possible [14,15], it is sufficient here to invoke the standard semi-classical justification [6,11,13] for the calculation procedure based on the radiation reaction viewpoint.

The classical equation of motion for a harmonically bound electron (charge e , mass m) corresponding to a dipole moment μ oscillating at frequency Ω' can be written in the secular approximation as

$$\frac{\partial \mu}{\partial t} = -i\Omega'\mu + \frac{e^2}{2m\Omega'} E_x(0), \quad (6)$$

where $E_x(0)$ is the x component of the electric field (i.e., parallel to the dipole moment) produced by the dipole at $x=y=z=0$ and evaluated at the same point. For an ansatz solution of the form

$$\mu = \mu_0 e^{-i\omega t} \quad (7)$$

we note that the real part of $E_x(0)$ contributes to a shift in the frequency of the dipole, while the imaginary part gives the decay constant. We now separate the electric field into two parts: E^D , the direct field that is produced when the dipole emits in the absence of a cavity (i.e., in

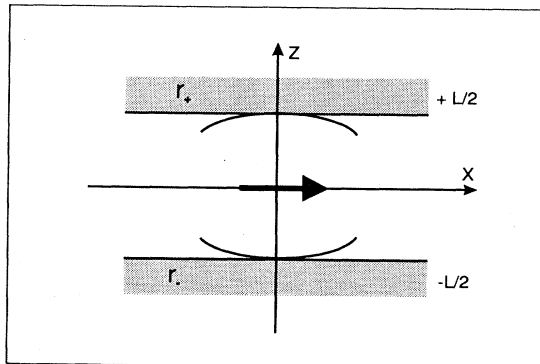


FIG. 2. Coordinate system for the calculation of the dipole emission. The dipole is placed at the origin and is directed along the x axis. The cavity (planar or confocal) has its axis in the z direction.

free space), and E^R , the additional contribution coming from the reflection on the cavity walls:

$$E_x(0) = E_x^D(0) + E_x^R(0). \quad (8)$$

With this partition, the equation of motion for the dipole can be written as

$$\frac{\partial \mu}{\partial t} = -i \left[\Omega - i \frac{\gamma_0}{2} \right] \mu + \frac{3c^3}{4\Omega^3 n_0} \gamma_0 E_x^R(0), \quad (9)$$

where

$$\gamma_0 = \frac{2e^2 \Omega^2 n_0}{3c^3 m} \quad (10)$$

is the energy decay rate that is produced by $E_x^D(0)$, while Ω incorporates the corresponding frequency shift. In this form, the equation of motion for the dipole moment addresses the problem of spontaneous emission in two steps: first, it deals with the emission of the dipole in free space, through the calculation of γ_0 , and second, it treats the modification of the emission rate by the presence of the boundary conditions of the cavity, through the calculation of the reflected field $E^R(0)$.

When this same calculation is carried out through a rigorous quantum-mechanical formulation of the radiation reaction viewpoint [14,17], the energy decay rate is obtained as

$$\gamma_0 = \frac{4n_0 \mu_0^2 \Omega^2}{3\hbar c^3}, \quad (11)$$

which is, of course, the value corresponding to the Einstein A coefficient. Thus Eq. (9) can be considered as incorporating the quantum-mechanical aspects of spontaneous emission through the appropriate expression for γ_0 . On the other hand, the presence of the term that arises from the modification of the boundary conditions [the last term in Eq. (9)] can be considered within a classical framework: In the course of spontaneous emission, the electric field that is reflected back onto the dipole site drives the dipole and modifies the quantum-mechanical spontaneous-emission rate. Thus the modification of the characteristics of spontaneous emission by the cavity walls can be addressed through a relatively simple calculation of the spatial distribution of the field, performed through one of the numerous methods developed in classical antenna theory.

To calculate these modifications when the semiconductor is in a single-mode cavity that presents a resonance at Ω of width κ , we examine the situation in which the cavity mode spans only a small solid angle when viewed from the site of the exciton, so that the dipole emission that occurs at off-axis angles is characterized by the free-space decay constant γ_0 . The amplitude of the electric field emitted into the mode and evaluated at $x=y=z=0$ can be approximated by a Lorentzian of the form

$$E_x^R(0) = \frac{\mu \Omega^2 / V}{\omega^2 - \Omega^2 + i\omega\kappa} \approx \frac{\mu \Omega / (2V)}{\omega - \Omega + i\kappa/2}, \quad (12)$$

where V is the effective volume of the cavity mode [11]. The complex frequency for the evolution of the dipole in

Eq. (9) is then given by the solution to the equation

$$\omega - \Omega + i \frac{\gamma_0}{2} = \frac{\mu_0^2}{\hbar} \frac{\Omega / (2V)}{\omega - \Omega + i\kappa/2} \quad (13)$$

and corresponds to the familiar Rabi doublet

$$\omega = \Omega \pm \left[g^2 - \left[\frac{\gamma_0 - \kappa}{4} \right]^2 \right]^{1/2} - i \left[\frac{\gamma_0 + \kappa}{4} \right], \quad (14)$$

where

$$g = \mu_0 \left[\frac{\Omega}{2\hbar V} \right]^{1/2} \quad (15)$$

is the radiative coupling constant for the dipole to the cavity mode. In obtaining Eq. (13) from Eq. (9) we have used the quantum-mechanical expression for γ_0 [Eq. (11)] to make contact with the notation conventionally used in calculating the vacuum Rabi splitting. At this point, we wish to point out the formal similarity between Eq. (4) and the real part of Eq. (13). In fact, one expression can be converted into the other simply by taking into account the relationship between the integrated intensity of the Lorentzian absorption spectrum S and the oscillator strength (or the transition dipole) of the absorber,

$$S = \alpha_0 \gamma_0 \pi = \left[\frac{N_0}{V} \right] \frac{\mu_0^2 \pi \Omega}{\hbar c}, \quad (16)$$

where N_0 is the number of absorbing particles in the volume V . Equation (4) gives the transmission and the reflection spectra of the cavity when probed by an on-axis electromagnetic wave, while Eq. (13) describes the dynamics of spontaneous emission of the excitons into a single-mode cavity. This similarity reflects the fact that, in a single-mode cavity, the mode that is being probed in Eq. (4) is precisely the same as the one that receives the spontaneous emission in Eq. (13). As we shall see in Sec. IV, this correspondence breaks down for multimode cavities.

When $g^2 \gg \kappa \gamma_0$, the Rabi splitting can be resolved in the absorption and the reflection spectra of the cavity and the radiative coupling is said to be strong. Under this condition in a single-mode cavity, then, the decay of the excitons occurs at a rate of $(\gamma_0 + \kappa)/2$, according to Eq. (14). This means that the kinetics of energy flow will be dominated by the largest one of the two decay rates: When $\kappa \gg \gamma_0$, most of the energy will flow into the decay channel of the cavity, that is, into the directional beam emerging from the cavity, rather than laterally, into the loss modes.

IV. SPONTANEOUS EMISSION IN PLANAR MICROCAVITIES

We now consider a planar cavity, consisting of two plane mirrors placed at $z = \pm L/2$ so as to be parallel to the xy plane (see Fig. 2). The complex reflectivities (for the field amplitude) of the two mirrors will be designated by r_{\pm} . As in Sec. II, we place a single dipole at $x = y = z = 0$ directed parallel to the x axis, representing the transition dipole of a quantum-well exciton.

The amplitude of the electric field at the site of the emitting dipole inside the cavity can be calculated through the standard methods of classical antenna theory. In particular, the problem of the radiation pattern of a dipolar antenna emitting in a stratified medium is treated in many textbooks on electromagnetic theory [18]. Such a calculation in connection with the problem of spontaneous lifetime modification was used quite early by Chance, Prock, and Silbey [13] and more recently applied to the case of light emitting diodes incorporating metallic mirrors [6]. In this mathematical procedure, the field emitted by the dipole is expressed in cylindrical coordinates (ρ, z, θ) as an integral over all wave vectors and the spatial distribution of the field in cavity can be calculated through the interferences due to the successive reflections on the cavity walls. At the origin, the total field (direct plus reflected) due to the TE waves, projected in the x direction (parallel to the emitter dipole moment), is given by [13,18]

$$E_x^{\text{TE}}(0) = \frac{i}{2} \left[\frac{\omega}{c} \right]^2 \mu \int_0^{\infty} \left\{ \frac{(1 + r_+^{\text{TE}} e^{ik_z L})(1 + r_-^{\text{TE}} e^{ik_z L})}{1 - r_+^{\text{TE}} r_-^{\text{TE}} e^{2ik_z L}} \right\} \times \frac{k_{\rho}}{k_z} dk_{\rho}, \quad (17)$$

where the radial (k_{ρ}) and the axial (k_z) components of the wave vector satisfy

$$k_{\rho}^2 + k_z^2 = n_0^2 \frac{\omega^2}{c^2}. \quad (18)$$

Similarly, for the total field along x due to the TM waves, we have

$$E_x^{\text{TM}}(0) = \frac{i}{2n_0^2} \mu \int_0^{\infty} \left\{ \frac{(1 + r_+^{\text{TM}} e^{ik_z L})(1 + r_-^{\text{TM}} e^{ik_z L})}{1 - r_+^{\text{TM}} r_-^{\text{TM}} e^{2ik_z L}} \right\} \times k_{\rho} k_z dk_{\rho}. \quad (19)$$

The factor in curly brackets in the integrands of Eqs. (17) and (19) results from the successive reflections of the field on the cavity walls and is essentially the Fabry-Pérot resonance function for the TE and the TM fields. In free space, this function is equal to 1, as can be seen by taking $r_{\pm} = 0$. Equations (17) and (19) can be interpreted as a summation over all directions of all components of the field propagating from the origin and being reflected back to the origin, including also evanescent components (whose wave vector is imaginary in the z direction), which are important for the determination of the near field. Clearly, if only one mode were allowed in the cavity (say, $k_{\rho} = 0$) there would be no integration and Eqs. (17) and (19) would give a result identical to Eq. (12) for the reflected part of the electromagnetic field, when the exponential in the denominator is expanded in the vicinity of a resonance ($k_z L \approx n\pi$). However, the presence of a continuum of modes with $k_{\rho} \neq 0$, whose individual contributions are summed in Eqs. (17) and (19), modifies

significantly the form of the field at the site of the emitting dipole.

We note that, in these equations, the nature of the mirrors is incorporated into a single quantity—the (TE or TM) complex reflectivity—and thus these equations can be readily applied to the calculation of the characteristics of spontaneous emission in nonideal, experimentally realizable cavities, such as the semiconductor microcavities involving Bragg mirrors used in the recent experiments [9,10]. However, since for multilayer Bragg mirrors the reflectivities r^{TE} and r^{TM} depend on k_ρ (that is, on the angle of incidence), such calculations are best carried out numerically.

Considerable insight into the spontaneous-emission characteristics in planar microcavities can be obtained, however, if Eqs. (17) and (19) are integrated analytically for a model in which the mirror reflectivity is independent of the angle of incidence. The simplest model that nevertheless reproduces the main features of the semiconductor microcavities in which the exciton splitting was observed would correspond to $r_+ = r_- \approx +1$. In this model, the two mirrors are taken to be identical, perfectly reflecting, and free from the off-axis optical leaks that characterize actual Bragg reflectors. The zero phase shift upon reflection in this model corresponds to neglecting the field penetration in the multilayer mirrors, with the cavity spacer being a high-refractive-index material (a π -phase shift would have been obtained with a low-refractive-index spacer). The TE and TM components of the field at the site of the emitting dipole reduce then to

$$E_x^{\text{TE}}(0) = \frac{i}{2} \left(\frac{\omega}{c} \right)^2 \mu \int_0^\infty \left\{ \frac{1+e^{ik_z L}}{1-e^{ik_z L}} \right\} \frac{k_\rho}{k_z} dk_\rho \quad (20)$$

and

$$E_x^{\text{TM}}(0) = \frac{i}{2n_0^2} \mu \int_0^\infty \left\{ \frac{1+e^{ik_z L}}{1-e^{ik_z L}} \right\} k_\rho k_z dk_\rho. \quad (21)$$

Operating a change of variables

$$u = \frac{ck_z}{n_0\omega}, \quad (22)$$

where u is essentially the cosine of the azimuthal angle of the wave vector, and limiting our calculation only to the imaginary part of the field (since it is this term that gives the radiative decay rate of the excitons in the microcavity), we have

$$\frac{\gamma}{2} = \text{Im} \left[-\frac{3}{8} i \gamma_0 \int_P (1+u^2) \left\{ \frac{1+e^{2\pi i \Lambda u}}{1-e^{2\pi i \Lambda u}} \right\} du \right], \quad (23)$$

where

$$\Lambda = \frac{n_0 L}{\lambda} \quad (24)$$

is the number of wavelengths that can fit in the cavity on axis. The path of integration P goes from $u = 1+i\delta$ to $u = 0+i\delta$ (slightly above the real axis) and then to $u = +\infty$. We note that the integrand of Eq. (23) has poles on the real axis, each time that

$$u = \frac{N}{\Lambda}, \quad (25)$$

where $N=0,1,2,\dots$ is a positive integer, including zero. Each of these poles represents a direction towards which the constructive interferences of the Fabry-Pérot make spontaneous emission allowed. As we are interested only in the imaginary part of the integral, we may subtract from it its complex conjugate (and divide by 2), which is essentially equivalent to adding the integration path indicated by P' in Fig. 3, closing the contour by a half-circle through $-\infty$ (indicated by C in Fig. 3), and multiplying the result by $\frac{1}{2}$. This contour integral can then be evaluated quite simply by finding the residues at all the poles. The decay rate for the field amplitude ($\gamma/2$) then is given by

$$\frac{\gamma}{2} = \frac{3\gamma_0}{8\Lambda} \left\{ \frac{1}{2} + \sum_{N=1}^{[\Lambda]} \left[1 + \frac{N^2}{\Lambda^2} \right] \right\} \quad (26)$$

$$= \frac{3\gamma_0}{16} \frac{2[\Lambda]+1}{\Lambda} + \frac{\gamma_0}{16} \frac{2[\Lambda]^3+3[\Lambda]^2+[\Lambda]}{\Lambda^3}, \quad (27)$$

where $[\Lambda]$ is the greatest integer part of Λ . The structure of this equation as a sum of $[\Lambda]+1$ terms permits us to distinguish the contribution of each direction in which constructive interferences make spontaneous emission possible in a Fabry-Pérot cavity. The first term

$$\frac{\Gamma_0}{2} = \frac{3\gamma_0}{16\Lambda} \quad (28)$$

comes from the pole at $u=0$ and gives the emission rate in the direction parallel to the cavity plane ($\theta_0=\pi/2$) into the guided modes that occur because of the high refractive index of the spacer. The $[\Lambda]$ other terms

$$\frac{\Gamma_N}{2} = \frac{3\gamma_0}{8} \left[\frac{1}{\Lambda} + \frac{N^2}{\Lambda^3} \right] \quad (29)$$

give the emission rate into each of the $[\Lambda]$ cones [of angle $\theta_N = \arccos(N/\Lambda)$] allowed in the Fabry-Pérot cavity. We note that for a cavity of width $L = \lambda_0$, resonant with

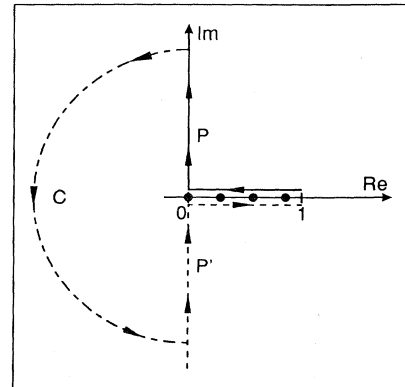


FIG. 3. Integration path for calculating the radiative decay rate of a dipole in a planar microcavity composed of a high-refractive-index spacer and low-refractive-index Bragg mirrors.

the exciton transition, 20% of the spontaneous emission goes to the in-plane guided modes.

A plot of Eq. (26), the overall spontaneous-emission rate as a function of the cavity length, is shown in Fig. 4 (solid line). This plot indicates that, even in the absence of losses in the mirrors, the excitons always decay radiatively into the continuum that consists of all the off-axis cavity modes. Clearly, this decay occurs even in the strong-coupling situation, in which a splitting of the exciton resonance is observable in the absorption or reflection spectrum. For cavity lengths smaller than λ_0/n_0 , emission can occur only into the guided modes and, within this simplistic model, the decay rate diverges as the cavity length tends to zero $L \rightarrow 0$. This situation, however, is never realized in a physical system as the field penetration in the Bragg mirrors prevents the effective cavity length from becoming too small. For cavity lengths greater than or equal to the wavelength ($L \geq \lambda_0/n_0$) emission occurs also in the direction perpendicular to the mirrors. However, the value of the radiative decay constant is of the order of γ_0 , the cavityless spontaneous-emission rate, displaying only a slight enhancement whenever the cavity length equals an integral number of wavelengths, the largest being a factor of 1.875 enhancement when $L = \lambda_0/n_0$.

The reason for which a planar microcavity, even lossless, will not give rise to a dramatic change in the spontaneous-emission dynamics can be understood through the following physical picture. The radiating dipole emits essentially spherical waves that in the course of the successive round-trips in the cavity, expand laterally so that the radiated energy is dissipated into the continuum of cavity modes with a nonzero in-plane wave vector. At the same time, the field amplitude reflected back to the emitting dipole decreases with each successive round-trip, producing a corresponding decrease in

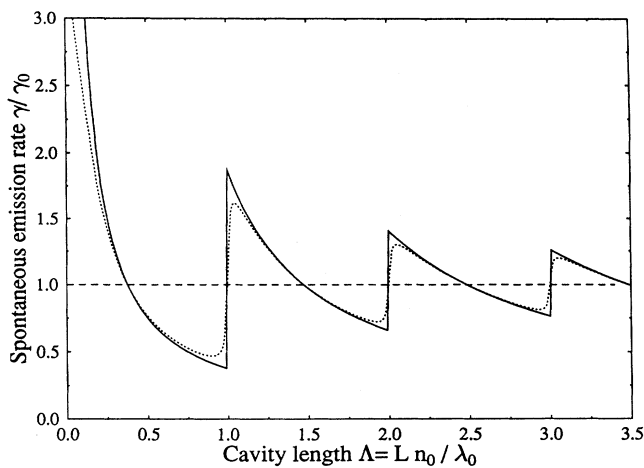


FIG. 4. Spontaneous-emission rate for an exciton in a planar microcavity composed of a high-refractive-index spacer and low-refractive-index Bragg mirrors, relative to the cavityless rate, as a function of the cavity length (in units of the wavelength). Solid line, lossless mirrors; dotted line, mirrors with 5% transmission; dashed line, cavityless emission rate.

the coupling between the dipole and the reflected field. By contrast, in a single-mode cavity with lateral confinement of the field, the energy radiated inside a narrow cone around the cavity axis remains in that cone so that the field reflected back to the emitting dipole is essentially constant throughout its successive round-trips between the cavity mirrors. In a single-mode cavity then, the coupling of the dipole to the reflected field gives rise to the familiar Rabi oscillations in which the energy is transferred periodically between the dipole and the cavity mode. A schematic of the situation in which the spontaneous emission of the exciton is channeled dissipatively to a planar cavity, according to the above analysis, is given in Fig. 5 and is clearly different from the situation in a single-mode cavity, in which the Rabi coupling produces a coherent oscillation of the energy between the two subsystems, shown in Fig. 1. Let us emphasize, however, that the observation of a Rabi splitting in transmission or reflection experiments [9,10] is not incompatible with the dissipative nature of the radiative coupling in planar microcavities. The reason is that in such experiments the probing beam is essentially a plane wave since its far-field divergence is smaller than the angular width of the microcavity resonance. Probing the microcavity response with a quasiparallel wave along a single direction gives no indication of its response to a spherical wave front initiated within the microcavity. On the other hand, if the collection of excitons (or atoms) in the microcavity has a substantial degree of mutual coherence so that the emission wave front approaches that of a plane wave (for example, if the excitons are created by a coherent light beam with planar wave front), it may then be possible to observe Rabi oscillations in a planar microcavity [19], analogous to those of a single-mode cavity.

Inclusion of cavity losses through a finite transmission for the mirrors (corresponding to reflectivities $r_+ = r_- = e^{-\tau/2}$ where the energy transmission τ is related to the energy decay constant by $\tau = \kappa L n_0 / c$) would change the Fabry-Pérot resonance function in the integrand of Eq. (23) to

$$\left\{ \frac{1 + e^{2\pi i \Lambda u - \tau/2}}{1 - e^{2\pi i \Lambda u - \tau/2}} \right\}. \quad (30)$$

This simply shifts the poles of the integrand vertically to $U_N = N/\Lambda - i(\tau/4\pi\Lambda)$, below the real axis, so that the

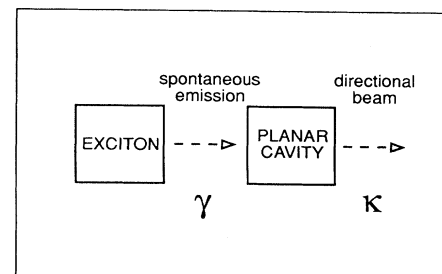


FIG. 5. Schematic representation of the flow of energy in the radiative emission of an exciton inside a planar microcavity: at all coupling strengths, the exciton decays dissipatively into the continuum of cavity modes.

path of integration P now passes a finite distance away from the poles. This makes the absolute value of the integral generally smaller and implies that, when the cavity mirrors have a finite transmission so that the field in the cavity can decay into a directional beam (or cone), the slight resonant enhancement of the spontaneous-emission rate will decrease. The overall decay constant will then approach γ_0 , the cavity-less spontaneous-emission rate, as seen in Fig. 4 (dotted line), where γ is evaluated numerically for $\tau=0.05$. This behavior contrasts with that of a single-mode cavity, in which the cavity decay constant may determine the dissipative part of the overall exciton-cavity system. Similar conclusions on the decrease of the cavity enhancement of the spontaneous-emission rate may be drawn by considering the drop of reflectivity that the Bragg reflectors display for angles away from the mirror axis.

V. SUMMARY AND CONCLUSIONS

The observation of a splitting in the absorption and the reflection spectra of planar semiconductor microcavities containing quantum-well excitons generally is not accompanied by a large modification of the spontaneous-emission rate of the excitons. The reason is that planar microcavities confine the electromagnetic field only in one dimension and thus possess a spectrally dense two-dimensional continuum of electromagnetic modes. Because of the presence of this continuum, an emitting dipole (such as an exciton) embedded in the cavity will decay radiatively at a rate close to the cavityless spontaneous-emission rate, even when its absorption and reflection spectra display a splitting characteristic of a

strong exciton-photon coupling.

This situation contrasts with the case of a single-mode cavity with lateral electromagnetic confinement in which the exciton level is coupled to a single discrete mode. In the strong-coupling regime, this gives rise to a coherent oscillatory exchange of the energy between the exciton and the cavity, so that the exciton-cavity coupled system can decay preferentially into the deexcitation channel of the cavity, if the decay constant is suitably adjusted.

From the point of view of technological applications, this analysis indicates that simple planar microcavities cannot be employed to bring about a significant modification of the spontaneous-emission characteristics of the excited material they contain, because of the existence of the spectral continuum in their modal structure. In order to be able to observe CQED effects associated with the strong-coupling conditions and the vacuum Rabi splitting, the spectral continuum should be "broken up" into a small number of sparsely spaced discrete modes, thus approximating the single-mode situation. This can be achieved by confining the field also in the two dimensions of the cavity plane either by lateral patterning of the semiconductor wafer (for example, by pixellation or by construction of a two-dimensional photonic band-gap structure) [4,12], or by building domelike spherical mirrors [20] on the microcavity structure.

ACKNOWLEDGMENT

This work was supported in part by an ESPRIT Basic Research Grant (No. 6934 QUINTEC) from the European Commission.

-
- [1] F. De Martini, M. Marrocco, P. Mataloni, L. Crescentini, and R. Loudon, *Phys. Rev. A* **43**, 2480 (1991); F. De Martini, M. Marrocco, P. Mataloni, D. Murra, and R. Loudon, *J. Opt. Soc. Am. B* **10**, 360 (1993).
 - [2] H. Khosravi and R. Loudon, *Proc. R. Soc. London Ser. A* **436**, 373 (1992).
 - [3] A. M. Vredenberg, N. E. J. Hunt, E. F. Schubert, D. C. Jacobson, J. M. Poate, and G. J. Zyzdik, *Phys. Rev. Lett.* **71**, 517 (1993).
 - [4] Y. Yamamoto, S. Machida, and G. Bjork, *Phys. Rev. A* **44**, 657 (1991); G. Bjork, S. Machida, Y. Yamamoto, and K. Igeta, *ibid.* **44**, 669 (1991); Y. Yamamoto, F. Matinaga, S. Machida, A. Karlsson, J. Jacobson, G. Bjork, and T. Mukai, *J. Phys. (France) II* **39**, (1993).
 - [5] D. G. Deppe and C. Lei, *J. Appl. Phys.* **70**, 3443 (1991).
 - [6] Z. Huang, C. C. Lin, and D. G. Deppe, *IEEE J. Quantum Electron.* **29**, 2940 (1993).
 - [7] S. D. Brorson, H. Yokoyama, and E. P. Ippen, *IEEE J. Quantum Electron.* **26**, 1492 (1990); H. Yokoyama, K. Nishi, T. Anan, Y. Nambu, S. D. Brorson, E. P. Ippen, and M. Suzuki, *Opt. Quantum Electron.* **24**, S245 (1992).
 - [8] S. T. Ho, S. L. McCall, and R. E. Slusher, *Opt. Lett.* **18**, 909 (1993).
 - [9] C. Weisbuch, M. Nishioka, A. Ishikawa, and Y. Aarakawa, *Phys. Rev. Lett.* **69**, 3314 (1992).
 - [10] R. Houdré, R. P. Stanley, U. Oesterle, M. Ilegems, and C. Weisbuch, *J. Phys. (France) II* **3**, 51 (1993).
 - [11] S. Haroche, in *Fundamental Systems in Quantum Optics*, 1990 Les Houches Lectures Session LIII, edited by J. Dalibard, J. M. Raymond, and J. Zinn-Justin (Elsevier Science, Amsterdam, 1992), p. 769.
 - [12] E. Yablonovitch, *J. Opt. Soc. Am. B* **10**, 283 (1993).
 - [13] R. R. Chance, A. Prock, and R. Silbey, *J. Chem. Phys.* **60**, 2744 (1974); **62**, 771 (1975); in *Advances in Chemical Physics*, edited by I. Prigogine and S. Rice (Wiley, New York, 1978), Vol. 37, p. 1.
 - [14] P. W. Miloni and W. A. Smith, *Phys. Rev. A* **11**, 814 (1975).
 - [15] I. Abram (unpublished).
 - [16] Yifu Zhu, D. J. Gauthier, S. E. Morin, Quilin Wu, H. J. Carmichael, and T. W. Mossberg, *Phys. Rev. Lett.* **64**, 2499 (1990).
 - [17] J.R. Ackerhalt, P. L. Knight, and J. H. Eberly, *Phys. Rev. Lett.* **30**, 456 (1973).
 - [18] J. A. Kong, *Electromagnetic Wave Theory* (Wiley-Interscience, New York, 1986).
 - [19] T. B. Norris, J. K. Rhee, C. Y. Sung, Y. Aarakawa, M. Nishioka, and C. Weisbuch, *Phys. Rev. B* **50**, 14663 (1994).
 - [20] F. M. Matinaga, A. Karlsson, S. Machida, Y. Yamamoto, T. Suzuki, Y. Kadota, and M. Ikeda, *Appl. Phys. Lett.* **62**, 443 (1993).